



by
Boehringer Ingelheim

KRAS G12C inhibitor

BI-0474

Table of contents

Summary	2
Chemical Structure.....	2
Highlights.....	3
Target information.....	3
In vitro activity.....	4
<i>In vitro</i> DMPK and CMC parameters	5
<i>In vivo</i> DMPK parameters.....	6
<i>In vivo</i> pharmacology	6
Negative control.....	8
Selectivity.....	8
Supplementary data	9
References.....	9

Summary

BI-0474 is a covalent KRAS^{G12C} inhibitor showing high cellular activity and *in vivo* efficacy after intraperitoneal administration. It was discovered using structure-based design approaches, by optimizing non-covalent binding of a fragment hit¹.

Chemical Structure

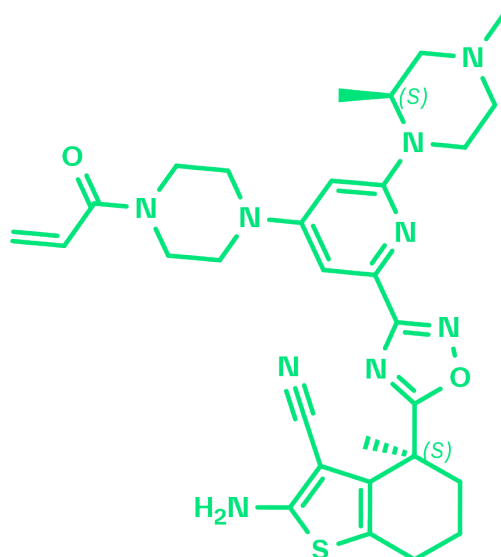


Figure 1: 2D structure of BI-0474, a covalent KRAS^{G12C} inhibitor.

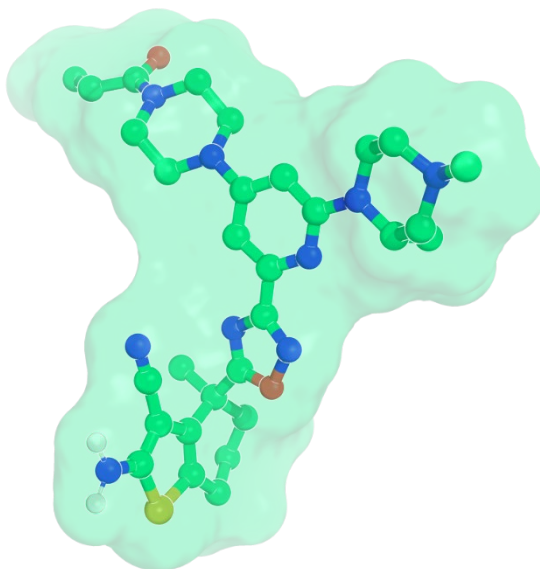


Figure 2: 3D conformation of BI-0474, based on the X-ray structure of the complex with KRAS^{G12C} (PDB code 8AFB)¹

Highlights

BI-0474 is an irreversible, covalent KRAS^{G12C} inhibitor showing high cellular activity and *in vivo* efficacy in an NCI-H358 xenograft model after intraperitoneal (ip) administration. BI-0474 has been discovered by Boehringer Ingelheim scientists in collaboration with the Fesik lab at Vanderbilt University, by optimizing non-covalent binding starting from a KRAS binder that was identified in an NMR-based fragment screen^{1,2}.

Target information

The KRAS oncoprotein is a GTPase acting as a key node in intracellular signaling pathways that are involved in cell growth and survival^{3,4}. In normal cells, KRAS functions as a molecular switch, alternating between an inactive GDP-bound and an active GTP-bound state⁵. Transition between these states is modulated by guanine-nucleotide exchange factors (GEFs) such as SOS, and GTP hydrolysis, which is catalyzed by GTPase-activating proteins (GAPs), to inactivate KRAS. GTP-bound KRAS allows binding of effector proteins to trigger downstream signaling pathways, including the RAF-MEK-ERK (MAPK) pathway⁶⁻⁹. Activating mutations in KRAS are the most frequent oncogenic driver events in cancer¹⁰. Oncogenic KRAS mutations have been shown to shift the equilibrium between the two KRAS states towards the active, GTP-bound form. However, the major oncogenic versions of KRAS still undergo GAP-mediated GTP/GDP exchange and reactivation¹¹. The oncogenic hotspot position 12, located at the lip of the switch II pocket, offers a covalent attachment point for KRAS^{G12C} inhibitors.

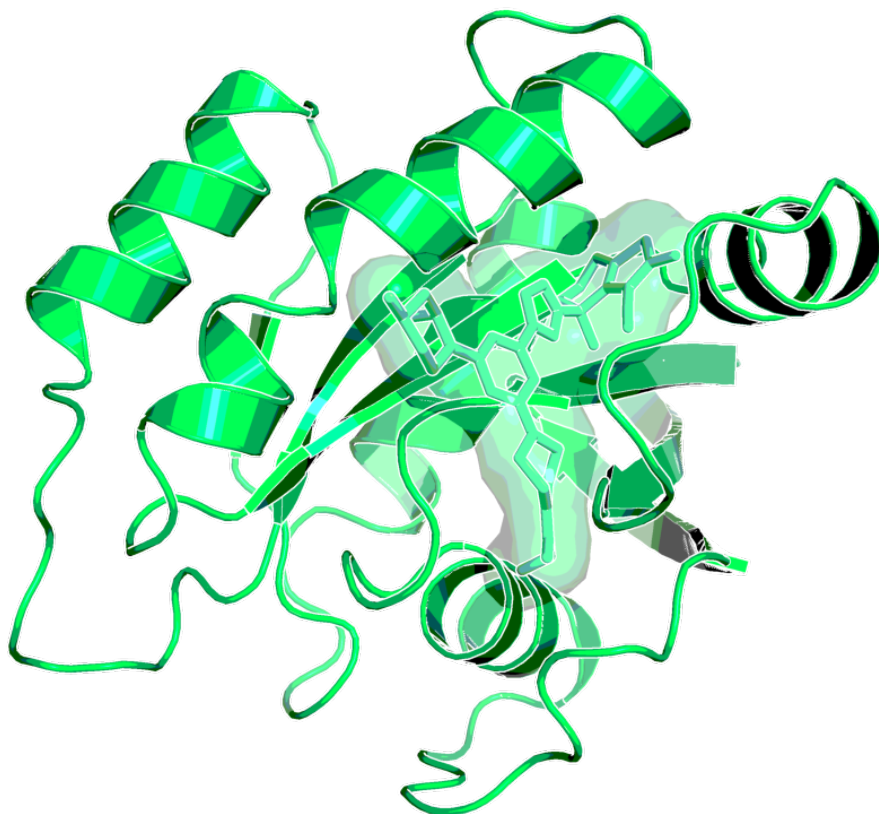


Figure 3: X-ray structure of the complex of BI-0474 with KRAS^{G12C} (PDB code: 8AFB)¹

In vitro activity

BI-0474 shows single digit nM biochemical activity in a KRAS^{G12C}::SOS1 PPI assay and an antiproliferative effect at low nM concentrations in KRAS^{G12C} mutated cell lines like NCI-H358. As BI-0474 is a KRAS^{G12C} selective covalent inhibitor, it only has μ M activity in the corresponding KRAS^{G12D} biochemical assay as well as μ M antiproliferative activity against a KRAS^{G12D} mutated cell line. The corresponding negative control shows almost 200-fold lower biochemical activity in the KRAS^{G12C}::SOS1 assay.

PROBE NAME / NEGATIVE CONTROL	BI-0474	BI-0473
MW [Da, free base] ^a	587.8	587.8
KRAS ^{G12C} ::SOS1 AlphaScreen (IC ₅₀) [nM] ^b	7	1,200
KRAS ^{G12D} ::SOS1 AlphaScreen (IC ₅₀) [nM] ^b	4,200	18,000
EC ₅₀ NCI-H358 proliferation [nM] ^c	26	n.d.
EC ₅₀ GP2D proliferation [nM] ^d	4,500	n.d.

^a For the salt form you will get, please refer to the label on the vial and for the molecular weight of the salt, please refer to the FAQs

^b BI-0474 is highly selective for KRAS^{G12C} compared to the KRAS^{G12D} mutant, as measured in vitro using an AlphaScreen assay. Details of the experimental procedure can be found in reference 1

^{c,d} BI-0474 shows potent antiproliferative activity on NCI-H358 cells carrying a G12C KRAS mutation. However, an antiproliferative effect on GP2D cells carrying a KRAS^{G12D} mutation was only observed in concentrations above 4 µM. Details of the experimental procedure can be found in reference 1

In vitro DMPK and CMC parameters

BI-0474 shows medium predicted clearance and a high Caco-2 efflux ratio.

PROBE NAME / NEGATIVE CONTROL	BI-0474	BI-0473
logD @ pH 11	3.2	3.2
Solubility @ pH 7 [µg/mL]	99	2
Caco-2 permeability AB @ pH 7.4 [$\times 10^{-6}$ cm/s]	0.8	n.a.
Caco-2 efflux ratio	45	n.a.
MDCK permeability P _{appAB} @ 1µM [10^{-6} cm/s]	0.4	n.a.
MDCK efflux ratio	72	n.a.
Microsomal stability (human/mouse/rat) [% Q _H]	73 / 53 / 59	76 / 61 / 72
Hepatocyte stability (human/mouse/rat) [% Q _H]	40 / 14 / -	- / 15 / -
Plasma Protein Binding (human/mouse/rat) [%]	96.7 / >98 / 98.3	- / 99.4 / -
CYP 3A4 (IC ₅₀) [µM]	15	n.a.

CYP 2C8 (IC ₅₀) [μM]	>50	n.a.
CYP 2C9 (IC ₅₀) [μM]	>50	n.a.
CYP 2C19 (IC ₅₀) [μM]	>50	n.a.
CYP 2D6 (IC ₅₀) [μM]	21	n.a.

In vivo DMPK parameters

BI-0474 shows decent exposure upon 25 mg/kg *p.o.* dosing as well as 50 mg/kg *i.p.* dosing (higher *i.p.* doses not tested). Oral dosing of 100 mg/kg did not lead to significantly increased exposure compared to 25 mg/kg.

BI-0474	MOUSE
Clearance [% Q _H] ^a	20
Mean residence time after <i>i.v.</i> dose [h] ^a	0.53
t _{max} [h] @ 42.5 μmol/kg ^b	2
C _{max} [nM] ^b	2,360
F [%]	23/24
V _{ss} [L/kg] ^a	0.6

^a *i.v.* dose mouse: 1 mg/kg (solution in 25% HP-β-CD, acidified with 0.1M HCl to pH 6)

^b *p.o.* dose mouse: 25 mg/kg (suspension in Natrosol 0.5% or methyl cellulose)

^c *i.p.* dose mouse: 50 mg/kg (solution in 25% HP-β-CD, acidified with 0.1M HCl to pH 6)

In vivo pharmacology

Target occupancy (TO) as well as pharmacodynamic (PD) biomarker modulation were assessed in the KRAS^{G12C} mutant NCI-H358 cell line-derived xenograft model after a daily treatment with 40 mg/kg *i.p.* on 3 consecutive days. As shown in Figure 4, MS-based TO analysis showed a strong and treatment-induced reduction of unmodified KRAS^{G12C} protein on the third day of consecutive treatment. This was confirmed by the analysis of RAS-GTP and p-ERK levels. Apoptosis induction was detectable in tumors in all 5 treated animals 6h post-dose on day 3, indicating that KRAS^{G12C} inhibition leads to induction of programmed cell death in this xenograft model. Anti-tumor efficacy was also assessed in this model, but as BI-0474 has not been optimized towards high oral bioavailability, it was administered *i.p.* once weekly or twice weekly on two consecutive days to explore whether infrequent systemic administration of

covalent KRAS^{G12C} inhibitors could be efficacious. At 40 mg/kg BI-0474 showed anti-tumor efficacy in both dose groups with 68 % and 98 % tumor growth inhibition (TGI), respectively. Both dose groups showed some body weight loss, which is less pronounced for the low dose group compared to the high dose group.

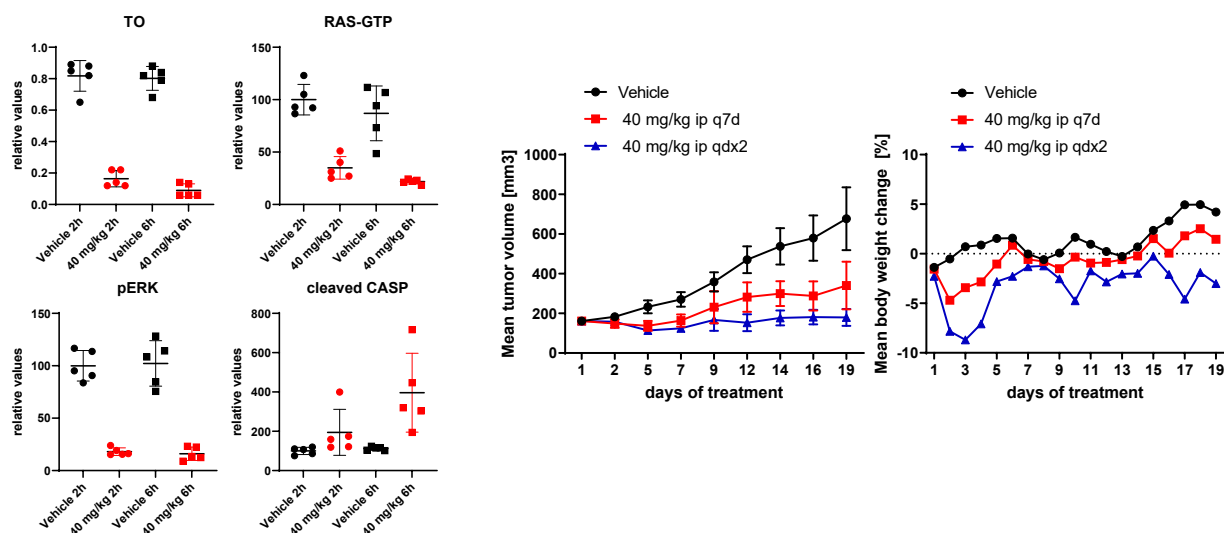


Figure 4: BI-0474 shows efficacy and PD biomarker modulation in an NCI-H358 cell line-derived non-small cell lung cancer xenograft model; left: treatment with BI-0474 leads to TO (decrease of unmodified KRAS^{G12C} protein levels measured by MS), reduction of RAS-G GTP and pERK levels, as well as apoptosis induction in vivo; right: BI-0474 shows efficacy in NCI-H358 xenograft (mean tumor volumes and mean body weight change shown vs. control (black circles), 40 mg/kg BI-0474 ip once/week (q7d, red squares), 40 mg/kg BI-474 ip twice/week on 2 consecutive days (qdx2, blue triangles); Details of the experimental procedures can be found in reference 1.

Negative control

The negative control BI-0473 is a diastereomer of BI-0474 and also carries an electrophilic acrylamide warhead. However due to the inverted stereo center close to the amino-cyanothiophene, which serves as one of the key pharmacophores, the non-covalent binding contribution is significantly reduced, resulting in a 200-fold lower biochemical activity compared to BI-0474.

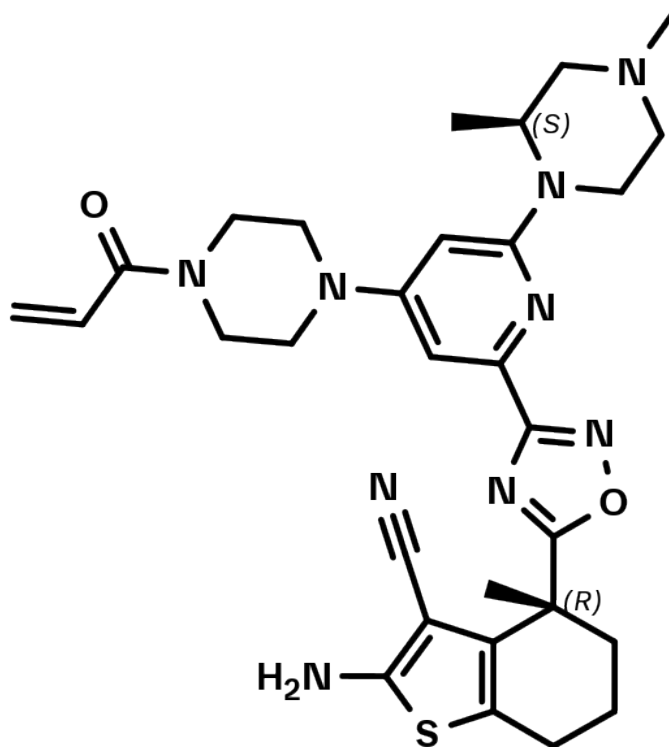



Figure 5: BI-0473 which serves as a negative control

Selectivity

As expected for a covalent KRAS^{G12C} inhibitor the compound shows a strong selectivity for KRAS^{G12C} vs other mutations (see KRAS^{G12C} vs. KRAS^{G12D} AlphaScreen data in the provided *in vitro* activity table). In the SafetyScreen44™ at a high concentration of 10 μM the compound hit 9 of 44 targets (M3/H, ALPHA1AH, COX-2, Ca+, MU/H, M2/H, COX-1, DATRANS, 5HT2B). Negative control BI-0473 hit 6 of 44 targets in SafetyScreen44™ at a high concentration of 10 μM (COX-2, KAPPA, 5HT2N, M2, COX-1, 5HT1B).

SELECTIVITY DATA AVAILABLE	BI-0474	BI-0473
SafetyScreen44™ with kind support of  eurofins	Yes	Yes
Invitrogen®	No	No
DiscoverX®	No	No
Dundee	No	No

Supplementary data

2D structure files can be downloaded free of charge from [openMe](https://openme.com).

References

- 1 Broeker J., Waterson A. G., Smethurst C., Kessler D., Böttcher J., Mayer M., Gmaschitz G., Phan J., Little A., Abbott J. R., Sun Q., Gmachl M., Rudolph D., Arnhof H., Rumpel K., Savarese F., Gerstberger T., Mischerikow N., Treu M., Herdeis L., Wunberg T., Gollner A., Weinstabl H., Mantoulidis A., Kraesaidmer O., McConnell D. B., Fesik S. W. Fragment Optimization of Reversible Binding to the Switch II Pocket on KRAS Leads to a Potent, In Vivo Active KRAS^{G12C} Inhibitor *J Med Chem* **2022**, 65 (21), 14614–14629. DOI: [10.1021/acs.jmedchem.2c01120](https://doi.org/10.1021/acs.jmedchem.2c01120), PubMed: [36300829](https://pubmed.ncbi.nlm.nih.gov/36300829/).
- 2 Sun Q., Phan J., Friber A. R., Camper D. M., Olejniczak E. T., Fesik S. W. A method for the second-site screening of K-Ras in the presence of a covalently attached first-site ligand *J Biomol NMR* **2014** 60, 11–14. DOI: [10.1007/s10858-014-9849-8](https://doi.org/10.1007/s10858-014-9849-8), PubMed: [25087006](https://pubmed.ncbi.nlm.nih.gov/25087006/).
- 3 Hofmann M. H., Gerlach D., Misale S., Petronczki M., Kraut N. Expanding the Reach of Precision Oncology by Drugging All KRAS Mutants *Cancer Discov.* **2022**, 12 (4), 924–937. DOI: [10.1158/2159-8290.CD-21-1331](https://doi.org/10.1158/2159-8290.CD-21-1331), PubMed: [35046095](https://pubmed.ncbi.nlm.nih.gov/35046095/).
- 4 Simanshu D. K., Nissley D. V., McCormick F. RAS Proteins and Their Regulators in Human Disease *Cell* **2017**, 170 (1), 17–33. DOI: [10.1016/j.cell.2017.06.009](https://doi.org/10.1016/j.cell.2017.06.009), PubMed: [28666118](https://pubmed.ncbi.nlm.nih.gov/28666118/).
- 5 Colicelli J. Human RAS superfamily proteins and related GTPases *Sci STKE* 2004, 2004(250), RE13. DOI: [10.1126/stke.2502004re13](https://doi.org/10.1126/stke.2502004re13), PubMed: [15367757](https://pubmed.ncbi.nlm.nih.gov/15367757/).
- 6 Freedman T. S., Sondermann H., Friedland G. D., Kortemme T., Bar-Sagi, D., Marqusee, S., Kuriyan J. A Ras-Induced Conformational Switch in the Ras Activator Son of Sevenless

- Proc National Acad Sci* **2006**, 103 (45), 16692–16697. [DOI: 10.1073/pnas.0608127103](#), [PubMed: 17075039](#).
- 7 Vigil D., Cherfils J., Rossman K. L. Der C. J. Ras Superfamily GEFs and GAPs: Validated and Tractable Targets for Cancer Therapy? *Nat Rev Cancer* **2010**, 10 (12), 842–857. [DOI: 10.1038/nrc2960](#), [PubMed: 21102635](#).
 - 8 Moore A. R., Rosenberg S. C., McCormick F., Malek S. RAS-Targeted Therapies: Is the Undruggable Drugged? *Nat Rev Drug Discov* **2020**, 19 (8), 533–552. [DOI: 10.1038/s41573-020-0068-6](#), [PubMed: 32528145](#).
 - 9 Boriack-Sjodin P. A., Margarit S. M., Bar-Sagi D., Kuriyan J. The Structural Basis of the Activation of Ras by Sos *Nature* **1998**, 394 (6691), 337–343. [DOI: 10.1038/28548](#), [PubMed: 9690470](#).
 - 10 Prior I. A., Hood F. E., Hartley J. L. The Frequency of Ras Mutations in Cancer *Cancer Res* **2020**, 80 (14), 2969–2974. [DOI: 10.1158/0008-5472.can-19-3682](#), [PubMed: 32209560](#).
 - 11 Lito P., Solomon M., Li L.-S., Hansen R., Rosen N. Allele-Specific Inhibitors Inactivate Mutant KRAS G12C by a Trapping Mechanism *Sci New York N Y* **2016**, 351 (6273), 604–608. [DOI: 10.1126/science.aad6204](#), [PubMed: 26841430](#).